Adhesion between Cerebroside Bilayers†

K. Kulkarni, D. S. Snyder, and T. J. McIntosh*

Department of Cell Biology, Duke University Medical Center, Durham, North Carolina 27710

Received July 26, 1999; Revised Manuscript Received September 17, 1999

ABSTRACT: The structure, hydration properties, and adhesion energy of the membrane glycolipid galactosylceramide (GalCer) were studied by osmotic stress/X-ray diffraction analysis.[1] Fully hydrated GalCer gave a repeat period of 67 Å, which decreased less than 2 Å with application of applied osmotic pressures as large as 1.6×10^9 dyn/cm^2. These results, along with the invariance of GalCer structure obtained by a Fourier analysis of the X-ray data, indicated that there was an extremely narrow fluid space (less than the diameter of a single water molecule) between fully hydrated cerebroside bilayers. Electron density profiles showed that the hydrocarbon chains from apposing GalCer monolayers partially interdigitated in the center of the bilayer. To obtain information on the adhesive properties of GalCer bilayers, we incorporated into the bilayer various mole ratios of the negatively charged lipid dipalmitoylphosphatidylglycerol (DPPG) to provide known electrostatic repulsion between the bilayers. Although 17 and 20 mol % DPPG swelled (disjoined) the GalCer bilayers by an amount predictable from electrostatic double-layer theory, 5, 10, 13, and 15 mol % DPPG did not disjoin the bilayers. By calculating the magnitude of the electrostatic pressure necessary to disjoin the bilayers, we estimated the adhesion energy for GalCer bilayers to be about -1.5 erg/cm^2, a much larger value than that previously measured for phosphatidylcholine bilayers. The observed discontinuous disjoining with increased electrostatic pressure and this relatively large value for adhesion energy indicated the presence of an attractive interaction, in addition to van der Waals attraction, between cerebroside bilayers. Possible attractive interactions are hydrogen bond formation and hydrophobic interactions between the galactose headgroups of apposing GalCer bilayers.

Both specific and nonspecific interactions between cell membranes determine the equilibrium separation between adjacent cells and play critical roles in a variety of biological processes in which cells come close together. For several years there has been an intense effort to measure and characterize the nonspecific interactions between bilayers composed of the main lipid components of biological membranes (see refs *1*−*5* for reviews). In particular, the repulsive pressures and/or total adhesion energies have been measured for bilayers composed of the main zwitterionic membrane phospholipids including phosphatidylcholine (*6*−*11*), phosphatidylethanolamine (*8, 12*−*14*), and sphingomyelin (*15*), as well as for several negatively charged membrane phospholipids, including phosphatidylglycerol, phosphatidylinositol, and phosphatidylserine (*16*−*18*). The effect of cholesterol on interbilayer interactions has also been extensively studied (*15, 19*). The interactions between most of these lipid bilayer systems have been characterized in terms of the attractive van der Waals interaction (*6, 7, 20*) and several repulsive pressures, including electrostatic repulsion (*16, 17*), hydration repulsion (*6, 7, 9*), and steric pressures due to molecular protrusions (*21, 22*) and bilayer undulations (*23*−*25*). In the case of phosphatidylethanolamine, the relatively large magnitude of the adhesion energy (*8, 12*) has been postulated to be the result of an additional attractive interaction due to direct electrostatic interbilayer interactions or indirect hydrogen-bonded water interactions between the NH_3^- groups in one bilayer and the PO_4^+ groups in the apposing bilayer (*14*).

Much less is known about the interactive and hydration properties of members of the other major class of lipids found in biological membranes, the glycolipids. Relatively high concentrations of glycolipids (20−30 mol %) are found in the plasma membranes of several cell types, particularly in the brain and the epithelium lining the intestines. The interactive properties of glycolipids are important because glycolipids are thought to have roles in cell−cell contacts (*26, 27*), cell−extracellular matrix interactions (*28, 29*), and the binding to membranes of ions, lectins, viruses, and toxins (*29*−*33*). Pressure−distance curves have been measured between bilayers containing mixtures of phospholipids and two types of glycolipids: (1) the negatively charged ganglioside GM1 (*34*) and (2) the uncharged lactosyl ceramide (*35*). For phospholipid:GM1 membranes there is long-range electrostatic repulsion as well as a short-range steric pressure arising from oligosaccharide headgroups that extend from apposing bilayer surfaces (*34*). Electrically neutral phospholipid:lactosylceramide bilayers also showed the presence of steric interaction, as well as a large adhesion energy, greater than that predicted by van der Waals attraction (*35*).

A glycolipid of particular physiological relevance is galactosyl ceramide (GalCer). GalCer, one of the simplest of the glycolipids as its headgroup contains a single saccharide, is a major lipid component of nerve myelin membranes

† Supported by grant GM-27278 from the National Institutes of Health.

* To whom correspondence should be addressed. Phone: 919-684-8950. Fax: 919-681-9929. E-mail: t.mcintosh@cellbio.duke.edu.

[1] Abbreviations: GalCer, galactosylceramide; PVP, poly(vinylpyrrolidone); DPPG, dipalmitoylphosphatidylglycerol; DPPC, dipalmitoylphosphatidylcholine; DPPE, dipalmitoylphosphatidylethanolamine; DLPE, dilauroylphosphatidylethanolamine.

10.1021/bi991725m CCC: $18.00
Published on Web 10/23/1999

and is thought to play a role in stabilizing the myelin membrane. Recently it has been shown that disrupted GalCer and cerebroside sulfate synthesis can lead to an increased membrane permeability, impaired packing of the myelin lipid bilayer, and a breakdown of saltatory conduction (*36*−*39*). GalCer can participate in carbohydrate−carbohydrate interactions (*40*−*42*) and has been shown in various neural cell lines to bind the HIV surface glycoprotein gp120 (*43*), suggesting a role for GalCer in HIV entry into neural cells (*43*).

Several previous studies have analyzed the hydration, thermal, and structural properties of synthetic and naturally occurring GalCers (bovine brain cerebrosides are primarily composed of GalCer). Synthetic and natural GalCer takes up significantly less water than zwitterionic phosphatidylcholines (*44*, *45*). Hydrated bilayers composed of either bovine brain ceramide (*46*, *47*) or several synthetic GalCers (*46*, *48*−*52*) have much higher chain melting transition temperatures than phospholipid bilayers of similar hydrocarbon chain composition. Several lines of evidence, including data from NMR (*53*), infrared spectroscopy (*54*), and X-ray crystallography (*55*, *56*), indicate the presence of intermolecular hydrogen bonds in the headgroup region of GalCer, and this H-bond network can help explain the high melting temperature of this lipid (*57*). Structural analysis of cerebroside crystals (*55*) show a H-bond network in the plane of the bilayer but no interbilayer H-bonding.

In this paper, we measure and analyze the interactions between hydrated bilayers composed of bovine brain GalCer to determine the adhesion energy and whether intermolecular hydrogen bonds or other short-range interactions between GalCer headgroups hold bilayers together and give rise to a large adhesion energy. Osmotic stress/X-ray diffraction experiments were performed on GalCer bilayers containing different concentrations of the charged phospholipid dipalmitoylphosphatidylglycerol (DPPG) which provides a predictable electrostatic repulsion to the bilayer (*14*). By determining the magnitude of the electrostatic energy necessary to disjoin the bilayers (*14*), we estimated the adhesion energy. Our experiments also provided information on the hydrocarbon packing in hydrated GalCer bilayers and indicated whether fully hydrated GalCer bilayers have interdigitated hydrocarbon chains such as those postulated for GalCer (*58*) and observed for other glycolipids (*59*). To provide additional information on the hydration properties of cerebroside bilayers, X-ray diffraction experiments were performed on anhydrous GalCer and on GalCer with ethyl alcohol. The effect of ethanol on GalCer structure was of interest since Yu et al. (*35*) argue that interbilayer hydrogen bonding may help explain the large adhesion energy measured for bilayers containing lactosylceramide, whereas an X-ray analysis of crystals with one molecule of ethanol per every two molecules of GalCer shows no interbilayer hydrogen bonding (*55*). However, X-ray diffraction (*48*, *60*), NMR (*61*), and Raman spectroscopy (*58*) indicate that there may be differences in structure between such ethanol-containing crystals and hydrated bilayers of GalCer.

MATERIALS AND METHODS

Bovine brain cerebrosides (primarily composed of GalCer) and the sodium salt of dipalmitoylphosphatidylglycerol (DPPG) were obtained from Avanti Polar Lipids, Inc. (Alabaster, AL). Dextran of average molecular weight 580 000 and poly(vinylpyrrolidone) (PVP) of average molecular weight 40 000 were purchased from Sigma Chemical Co. (St. Louis, MO).

X-ray Diffraction/Osmotic Stress. X-ray diffraction analysis was performed on both unoriented suspensions of multiwalled vesicles and oriented multilayers of various mixtures of cerebrosides and DPPG. For preparation of both types of samples, the appropriate lipid mixtures were first codissolved in 2:1 chloroform:methanol and then rotary evaporated to dryness. For some experiments the evaporated film was then placed in a high vacuum for 12 h to ensure the removal of residual solvent. This additional vacuum-drying step had no effect on the recorded diffraction patterns. To prepare oriented multilayers, the dry lipid mixture was hydrated in excess water by incubation at 80 °C for several hours. A small drop of the lipid suspension was then placed on a curved glass substrate and equilibrated overnight at 75% relative humidity. Unoriented suspensions were prepared by hydrating the rotary-evaporated lipid films with excess quantities (greater than 95 wt %) of 100 mM NaCl, 20 mM Hepes, pH 7 buffer, or polymer solutions made with various concentrations of dextran or PVP in the same buffer. To ensure complete hydration and equilibration of the salt across the multilayers (*62*), the lipid suspensions were incubated for three cycles of 30 min each at 80 °C (above the lipid's phase transition temperature) and then ambient temperature for 30 min.

For X-ray diffraction analysis, the multilayers on the glass substrate were mounted in a controlled humidity chamber on a single-mirror (line-focused) X-ray camera such that the X-ray beam was oriented at a grazing angle relative to the multilayers (*10*, *19*). The humidity chamber, which contained a cup of the saturated salt solution, consisted of a hollow-walled copper canister with two Mylar windows for passage of the X-ray beam. To speed equilibration, a gentle stream of nitrogen was passed through a flask of the saturated salt solution and then through the chamber. The unoriented suspensions were pelleted with a bench centrifuge, sealed in quartz glass X-ray capillary tubes, and mounted in a point collimation X-ray camera. All diffraction patterns were recorded at ambient temperature.

Known osmotic pressures were applied to each of these systems by published procedures (*6*, *9*, *10*, *63*). Pressure was applied to oriented multibilayers by incubating them in constant relative humidity atmospheres maintained with saturated salt solutions (*64*). The applied pressure is given by

$$P = -(RT/V_w) \ln(p/p_o) \quad (1)$$

where R is the molar gas constant, T is the temperature in Kelvin, V_w is the partial molar volume of water, p is the vapor pressure of the saturated salt solution, and p_o is the vapor pressure of water (*63*). Osmotic stress was applied to the unoriented suspensions with various concentrations of dextran or PVP. Since these polymers are too large to enter the lipid lattice, they compete for water with the lipid multilayers, thereby applying an osmotic pressure (*6*, *63*). Osmotic pressures for dextran and PVP solutions have been published (*65*).

For both oriented and unoriented specimens, X-ray diffraction patterns were recorded on Kodak DEF X-ray film. The films were processed by standard techniques and densitometered with a Joyce-Loebl microdensitometer as described previously (*9*, *10*, *19*). After background subtraction, integrated intensities, $I(h)$, were obtained for each order h by measuring the area under each diffraction peak. For unoriented patterns, the structure amplitude $F(h)$ was set equal to $\{h^2I(h)\}^{1/2}$ (*66*, *67*). For the oriented line-focused patterns, the intensities were corrected by a single factor of h due to the cylindrical curvature of the multilayers (*66*, *67*) so that $F(h) = \{hI(h)\}^{1/2}$.

Electron density profiles, $\rho(x)$, on a relative electron density scale were calculated from

$$\rho(x) = (2/d)\sum \exp\{i\phi(h)\}F(h)\cos(2\pi xh/d) \qquad (2)$$

where x is the distance from the center of the bilayer, d is the lamellar repeat period, $\phi(h)$ is the phase angle for order h, and the sum is over h. Phase angles were determined by the use of the sampling theorem (*68*) as described in detail previously (*19*, *69*). Electron density profiles are at a resolution of $d/2h_{max} \approx 7$ Å.

RESULTS

X-ray/Osmotic Stress Data. At 20 °C, for all hydrated GalCer:DPPG mixtures studied, the wide-angle X-ray pattern contained a single sharp reflection centered at 4.18 Å, consistent with lipids in a gel phase (*70*). The low-angle X-ray spacings depended on the amount of DPPG present in the sample. For fully hydrated GalCer suspensions containing 0, 5, 10, 13, and 15 mol % DPPG, the low-angle patterns consisted of several sharp reflections that indexed as multiple orders of a lamellar repeat period of 66−67 Å, indicating the presence of stacked bilayers. The repeat period for fully hydrated cerebroside was similar to that recorded by Abrahamsson et al. (*60*). For the sample containing 15 mol % DPPG, there were also weak broad bands centered at 60 and 27 Å. For fully hydrated GalCer samples containing 17, 20, or 25 mol % DPPG, the low-angle pattern contained no sharp reflections but rather consisted of broad bands centered at 60, 27, and 18 Å.

Osmotic stress-X-ray diffraction experiments were performed to obtain additional information on the structure and interactive properties of the GalCer:DPPG bilayers. For applied osmotic pressures (P) greater than 3×10^4 dyn/cm^2, each GalCer:DPPG sample containing 0−25 mol % DPPG gave low-angle X-ray patterns with sharp reflections that indexed as multiple orders of a lamellar repeat period. The samples containing 17, 20, or 25 mol % DPPG swelled to much larger repeat periods than those containing 0−15% mol % DPPG. Figure 1 shows a plot of the logarithm of applied pressure versus the lamellar repeat periods for GalCer:DPPG bilayers containing 0, 10, 17, and 20 mol % DPPG. The repeat period for GalCer:DPPG bilayers containing 17 and 20 mol % DPPG decreased from values greater than 100 Å at low applied pressure ($P < 1 \times 10^5$ dyn/cm^2, log $P < 5$) to 63 Å at the highest applied pressure of 1.6×10^9 dyn/cm^2 (log $P = 9.2$). For the pressure range $4 <$ log P < 7, the repeat period decreased exponentially with increasing applied pressure (solid line in Figure 1). However, for log $P > 7$, there was a sharp upward break in the pressure−distance relation. For cerebroside bilayers containing either 0 or 10 mol % DPPG, the repeat period decreased only slightly, from 67 Å in the absence of applied pressure to 65 Å at the highest applied pressure (log $P = 9.2$).

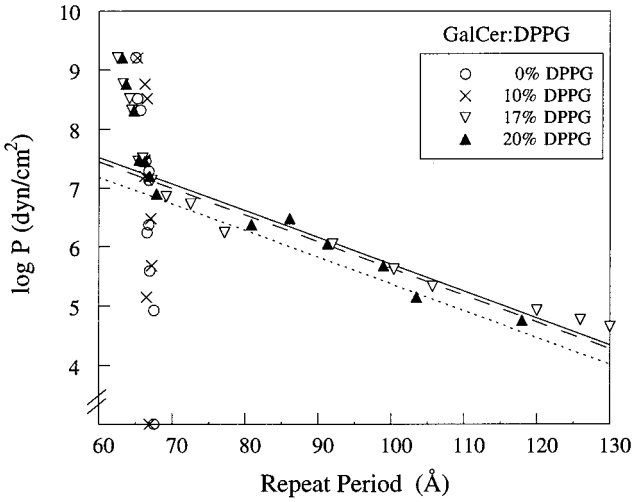

FIGURE 1: Natural logarithm of applied pressure (log P) plotted versus lamellar repeat period for unoriented suspensions (log $P <$ 7.5) and oriented multilayers (log $P >$ 7.5) of cerebroside bilayers containing 0, 10, 17, and 20 mol % DPPG. The data points shown on the x-axis were obtained from GalCer:DPPG liposomes containing 0 and 10 mol % DPPG in excess buffer with no applied pressure. (GalCer bilayers containing 13 and 15 mol % DPPG had similar repeat periods in excess buffer.) The solid, dashed, and dotted lines represent the electrostatic repulsion expected from double-layer theory between bilayers containing 20, 17, and 10 mol % DPPG, respectively (see text for details).

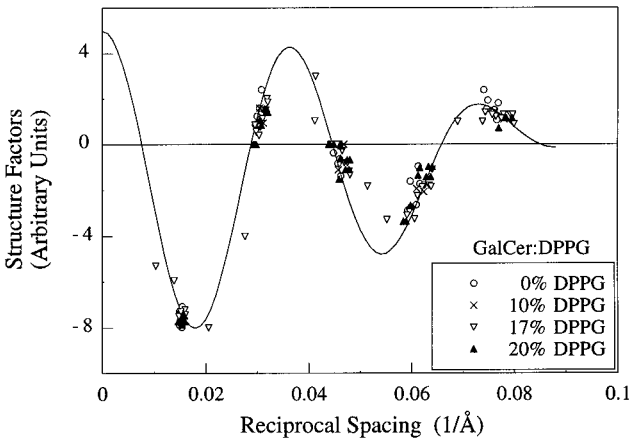

FIGURE 2: Structure factors plotted versus reciprocal spacing for cerebroside bilayers containing 0, 10, 17, and 20 mol % DPPG. The solid line is the continuous transform calculated from the sampling theorem for GalCer containing 0 mol % DPPG.

Analysis of X-ray Data. The lamellar repeat period represents the width of one unit cell which contains one bilayer and the fluid space between apposing bilayers. A Fourier analysis of the diffraction data was performed to obtain information on both the structure of the bilayer and the width of the fluid layer. Figure 2 shows the structure factors for GalCer:DPPG samples containing 0, 10, 17, and 20 mol % DPPG obtained from the osmotic stress experiments. The solid line is the continuous Fourier transform of the GalCer bilayer. This transform was calculated using the data set for log $P = 8.3$ and the phase combination which produced a transform that best fit the other data sets. There are three points worth noting about this transform. First, the

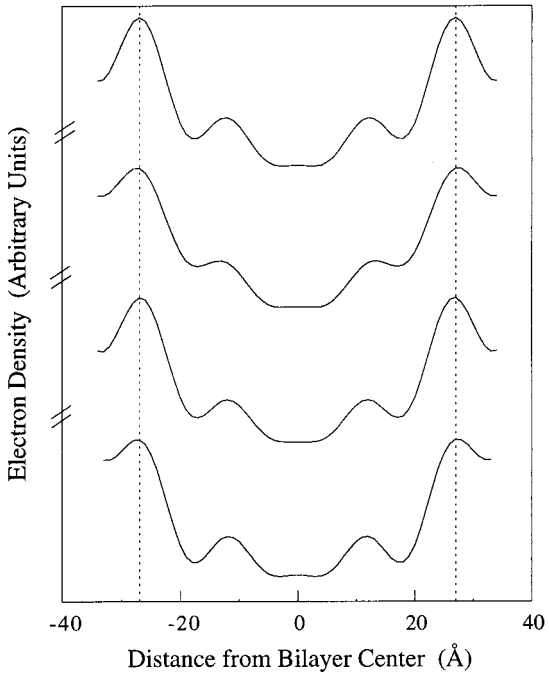

FIGURE 3: Electron density profiles for cerebroside bilayers for a range of applied pressures. From the top to the bottom profiles, the applied pressures were 0, 2.3×10^6, 1.6×10^7, and 1.6×10^9 dyn/cm^2. In each profile, one unit cell is shown. The vertical dotted lines are drawn through the middle of the headgroup peaks of the top profile recorded in excess buffer with no applied pressure.

amplitude peaks were at reciprocal spacings of 0.018, 0.037, and 0.055 Å^{-1}. These peak positions corresponded quite closely to the positions of the broad bands at 60, 27, and 18 Å observed in patterns from fully hydrated GalCer:DPPG with 17 and 20 mol % DPPG. Thus, the spacings of the broad bands corresponded to the first three peaks in the continuous Fourier transform of a bilayer, indicating that for the GalCer:DPPG mixtures containing more than 17 mol % DPPG the charged DPPG had disjoined the bilayers (*14*). Second, the structure factors for all of the samples with 0−20 mol % DPPG fell quite closely to this continuous transform, indicating that the incorporation of up to 20 mol % DPPG did not appreciably change the organization of the cerebroside bilayer. Third, the structure amplitudes from bilayers for all osmotic pressures fell closely to the transform, indicating that the structure of the bilayer did not appreciably change with increasing applied pressure.

Electron density profiles for cerebroside bilayers over a range of applied pressures are shown in Figure 3. The center of each profile is at the origin. The low electron density region in the center of each profile corresponds to the hydrocarbon core of the bilayer, the peaks located at ± 27 Å correspond to the polar headgroups, and the medium density regions at the edge of the profile correspond to the fluid space between bilayers. The shape of the bilayer portion of the profile did not appreciably change with increasing osmotic pressure. In particular, the separation of headgroup peaks across the bilayer (dotted lines in Figure 3) stayed nearly constant; the headgroup peak to headgroup peak separation was 53.9 ± 0.9 Å (mean ± standard deviation, $n = 8$ experiments). The only systematic difference among the profiles was that the electron density at the outer edge of the bilayer increased with increasing applied pressure. This can be more easily seen in profiles containing two unit cells,

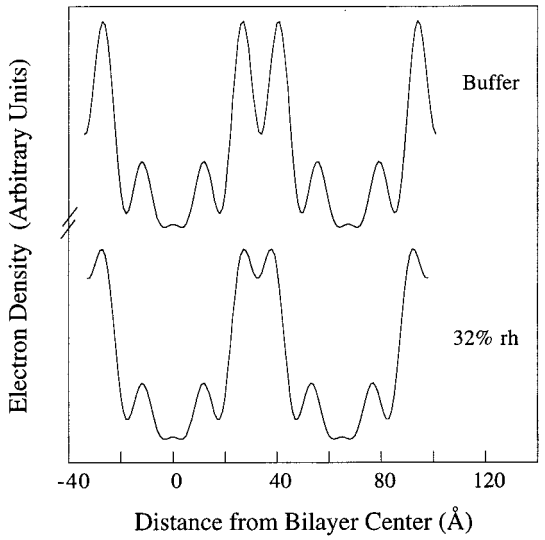

FIGURE 4: Electron density profiles for cerebroside bilayers obtained in excess buffer (top profile) and at 1.6×10^9 dyn/cm^2 (32% relative humidity). In each profile two unit cells are shown, with two bilayers and the fluid space between apposing bilayers.

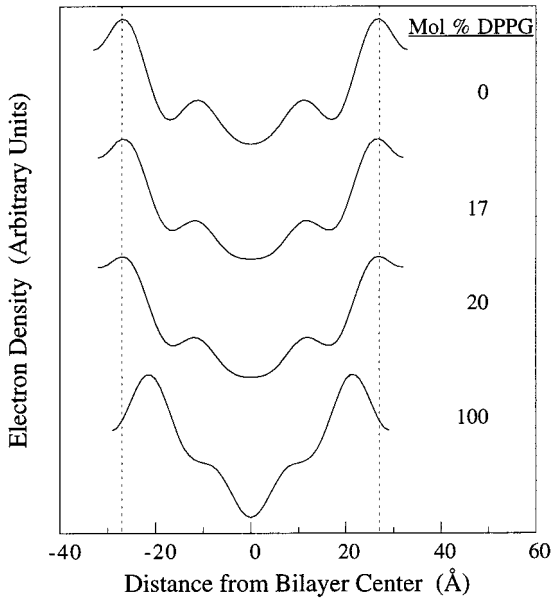

FIGURE 5: Electron density profiles for cerebroside:DPPG bilayers containing 0, 17, 20, and 100 mol % DPPG obtained at the same applied pressure (log $P = 8.5$). Each profile contains one unit cell. The vertical dotted lines were drawn through the headgroup peaks of the top profile of the cerebroside bilayer.

with two bilayers and the fluid space between apposing bilayers (Figure 4). The profiles in Figure 4 are from cerebroside bilayer at zero applied pressure and at the maximum applied pressure (log $P = 9.2$ obtained at 32% relative humidity). With increasing pressure, the distance between headgroup peaks from apposing bilayers decreased while the electron density between headgroup peaks from apposing bilayers increased.

Figure 5 shows profiles obtained from GalCer:DPPG bilayers containing 0, 17, 20, and 100% DPPG. The profile for 100% DPPG was similar to one previously obtained for gel-phase DPPG (*71*). The headgroup peak separation and shape of the profile were similar for cerebroside bilayers containing 0, 17, and 20 mol % DPPG. The headgroup peak separation was similar for the three mixtures, being 54.3 ±

0.9 ($n = 8$ experiments), 53.4 ± 1.3 ($n = 6$), and 54.0 ± 1.4 Å ($n = 4$) for cerebroside bilayers containing 0, 17, and 20 mol % DPPG, respectively. However, the profile for 100% DPPG differed in two ways: (1) the headgroup peak separation across the bilayer was considerably smaller (43 Å) and (2) there was a much sharper and deeper dip in electron density in the middle of the bilayer. The small peak-to-peak separation in pure DPPG bilayers is due to chain tilt of the hydrocarbon chains (*71*, *72*).

X-ray diffraction patterns were recorded from anhydrous GalCer and GalCer solvated with ethanol. Anhydrous cerebroside gave an X-ray pattern containing two wide-angle bands at 4.18 and 4.62 Å and four low-angle reflections that indexed as the first four orders of a lamellar phase with a repeat period of 65 Å. The intensity distribution and electron density profile of the anhydrous GalCer (data not shown) were similar to that of GalCer at 32% relative humidity. The X-ray pattern of GalCer in excess anhydrous ethanol contained several orders of a lamellar repeat period of 51 Å and several wide-angle spacings, the most intense being a sharp reflection at a spacing of 4.50 Å.

DISCUSSION

The results in these studies provide information on cerebroside bilayer structure, interbilayer interactions, and hydration properties.

Bilayer Structure. The X-ray diffraction data provide several pieces of information on the structure of GalCer multibilayers. First, the wide-angle patterns show that at 20 °C the cerebroside bilayers are in a gel phase with hexagonal packing of the hydrocarbon chains. Several previous calorimetry studies have shown that hydrated bovine brain cerebrosides melt at about 70 °C (*47*, *50*, *60*, *73*). Second, the structure factors (Figure 2) and electron density profiles (Figures 3 and 4) show that partial removal of water from these bilayers by osmotic stress has little effect on the bilayer structure. Such invariance in structure with partial dehydration has been found also with gel-phase phosphatidylcholine (*9*) and sphingomyelin (*15*) bilayers. Third, the wide-angle data, structure factors (Figure 2), and electron density profiles (Figure 5) indicate that the incorporation of up to 20 mol % DPPG into the cerebroside bilayers has little effect on bilayer organization. Fourth, the very different repeat periods and wide-angle spacings measured for GalCer in water and in ethanol are relevant to comparisons of the structure found for single crystals of synthetic GalCer (*55*) and the organization of GalCer in hydrated membranes. The GalCer crystals, which contained a 2:1 mol ratio of lipid to ethanol, gave a very small repeat (46 Å), due primarily to a very large tilt (49°) of the hydrocarbon chains with respect to the polar boundary (*55*). The chain tilt must be considerably less in our hydrated GalCer bilayers to account for the relatively large bilayer thickness (about 66 Å, see below). Abrahamsson et al. (*60*) also found a different hydrocarbon chain arrangement for a synthetic cerebroside (*N*-octadecanoylpsychosine) in the presence of water and in crystals grown from ethanol. Thus, since water and ethanol have quite different effects on the packing of GalCer, some of the atomic details found in crystals formed from ethanol, such as specific inter- and intramolecular hydrogen bond formation, might not be applicable to hydrated GalCer bilayers.

The electron density profiles provide further information on the packing of the hydrocarbon chains in the bilayer. GalCer bilayers containing 0−20 mol % DPPG show a much broader electron density dip in the center of the bilayer than the relatively deep, narrow trough observed in profiles at the same resolution of gel bilayers composed of diacyl phospholipids with two identical hydrocarbon chains, such as DPPG (Figure 5), dilauroylphosphatidylethanolamine (DLPE) (*74*), or dipalmitoylphosphatidylcholine (DPPC) (*9*, *75*, *76*, *77*). This indicates that in GalCer bilayers the low electron density terminal methyl groups of the hydrocarbon chains are not as well localized in the center of the bilayer as they are in gel-phase DPPG, DLPE, or DPPC bilayers. A likely reason for this is that in the cerebroside molecule the hydrocarbon chains are of unequal length, leading to a partial hydrocarbon chain interdigitation between apposing monolayers of the bilayer. That is, in bovine brain cerebrosides the most common fatty acid is 24 carbons long with no double bonds (24:0), which must cross the middle of the bilayer, whereas the short-chain sphingosine chain is not long enough to reach the bilayer center. Such partial hydrocarbon chain interdigitation has also been observed by X-ray diffraction (*59*) and infrared spectroscopy (*78*) in cerebroside sulfate bilayers and by spin label studies in several glycosphingolipids with asymmetric hydrocarbon chain lengths (*79*, *80*), as well as in phospholipids with asymmetric chains (*81*, *82*). In addition, in brain GalCer there is a mixture of acyl chain lengths, varying from 16:0 to 26:0, which could also contribute to the delocalization of the terminal methyl groups from the bilayer center.

Interbilayer Interactions. For gel-phase bilayers where the undulation (*11*, *24*, *25*) pressure is small, the repulsive pressure between charged phospholipid bilayers contains components due to hydration repulsion (*6*, *9*, *63*), steric interactions between apposing bilayers (*10*, *19*), and electrostatic repulsion (*16*, *83*, *84*).

With the assumptions of a constant potential and no counterion binding, the repulsive electrostatic pressure between two planar charged surfaces in a 1:1 electrolyte can be expressed as

$$P_{es} = 64kT\rho\gamma^2 \exp(-KD) \qquad (3)$$

where k is the Boltzmann constant, T is temperature, ρ is the bulk ionic concentration, $\gamma = \tanh(e\psi/4kT)$ where e is the electronic charge and ψ is the bilayer surface potential, $1/K$ is the Debye length (9.6 Å for 100 mM NaCl), and D is the distance between the charged layers (*84*). The surface potential can be calculated from the Gouy equation

$$\sinh(e\psi/2kT) = \sigma/(8\epsilon\epsilon_o kT\rho)^{1/2} \qquad (4)$$

where σ is the surface charge density, ϵ is the dielectric constant, and ϵ_o is the permittivity of free space (*85*). The surface charge density is estimated assuming that each DPPG molecule carries one negative charge, each cerebroside molecule is uncharged, and that the lipid area per molecule is twice the area per lipid chain, $A_c = 2(d_s)^2/(3)^{1/2}$, where d_s is the wide-angle spacing (*70*). For the origin of the electrostatic pressure ($D = 0$) for GalCer:DPPG bilayers, we estimate the position of the charged phosphate groups

from the position of the headgroup peak in the electron density profiles (Figure 5).

The electrostatic repulsive pressures calculated with these procedures for cerebroside bilayers containing 10, 17, and 20 mol % DPPG are shown in Figure 1. For cerebroside bilayers containing either 17 or 20 mol % DPPG, the pressure−distance data for $d > 66$ Å are very well matched by the electrostatic double-layer (eq 3) predictions. For $d <$ 66 Å (and log $P > 7$), for both 17 and 20 mol % DPPG systems, there are sharp upward breaks in the pressure−distance curves, away from the electrostatic predictions. These upward breaks undoubtedly are due to the bilayers coming into steric contact, as previously been demonstrated for both phospholipid and phospholipid:ganglioside bilayers (*10*, *34*). This implies that the width of these cerebroside:DPPG bilayer is about 66 Å. At the highest applied pressures, the repeat periods for GalCer bilayers containing 17 or 20 mol % DPPG are 1 to 2 Å smaller than from bilayers containing 0 or 10 mol % DPPG. A possible explanation for this is that the incorporation of DPPG decreases the surface density of the GalCer headgroups in the plane of the bilayer, thereby decreasing the range of the steric repulsion between apposing bilayers. A similar phenomenon has been observed in ganglioside bilayers containing increasing concentrations of PC (*34*). Thus, the entire pressure−distance relations for cerebroside bilayers containing 17 and 20 mol % DPPG can be explained in terms of two repulsive interactions, a short-range steric pressure and a longer-ranged electrostatic repulsive pressure.

In the case of bilayers containing 10 mol % DPPG (Figure 1), for log $P < 7$ the pressure−distance data do not agree with the electrostatic prediction but rather superimpose with the data from uncharged cerebroside bilayers (Figure 1). That is, 10 mol % DPPG does not provide enough electrostatic repulsion to disjoin or swell the cerebroside bilayers apart. Moreover, the repeat period of the cerebroside bilayers containing 0−10 mol % DPPG decreased only about 2 Å over the entire range of applied pressures ($0 < P < 1.6 \times 10^9$ dyn/cm^2), indicating that very little interbilayer water was removed. These results are similar to those reported for gel-phase dipalmitoylphosphatidylethanolamine (DPPE) bilayers (*14*). For comparison, over this range of applied pressures the repeat period of gel-state bilayers of DPPC is reduced about 8 Å (*11*). Moreover, gel-phase DPPC bilayers completely disjoin with the addition of only 5 mol % of charged lipid (*14*), whereas fully hydrated DPPE bilayers do not disjoin until 10 mol % charged lipid is added (*14*). Thus, fully hydrated cerebroside bilayers, like DPPE bilayers, have very narrow interbilayer fluid spaces in excess buffer and disjoin discontinuously with the addition of increasing amounts of charged lipid (electrostatic repulsion).

The pressure−distance data (Figure 1) can be used to estimate the adhesion energy between apposing cerebroside bilayers by the procedure we have used for DPPE bilayers (*14*). Our results indicate that the addition of 17 mol % DPPG provided just enough charge to disjoin the GalCer bilayers (Figure 1). Therefore, we use the electrostatic pressure for GalCer with 17 mol % DPPG calculated from eq 3 (Figure 1) as a measure of the minimum repulsive pressure necessary to disjoin GalCer bilayers. By integration of this line from infinite bilayer separation to the separation in excess buffer, we obtain the adhesion energy per unit area of $E \approx -1.5$ erg/cm^2. This estimated value of adhesion energy is large compared to values of adhesion energy for gel-phase phospholipid bilayers measured either with this osmotic stress method or with the surface force apparatus. For example, a value of -0.7 erg/cm^2 was obtained for DPPE with the osmotic stress method (*14*), and values of -0.8 erg/cm^2 for DPPE and -0.15 erg/cm^2 for DPPC were obtained with the surface force apparatus (*8*). Surface force apparatus measurement also gave an adhesion energy of -3.5 erg/cm^2 for ditridecanoylphosphatidylcholine containing 30 mol % of the disaccharide-containing sphingolipid lactosylceramide (LacCer) (*35*). Thus, although there are several assumptions involved in our calculation of the adhesive energy, the evidence is strong that bilayers containing the gel-phase glycosphingolipids GalCer or LacCer have significantly larger adhesion energies than do gel-phase PC or PE bilayers.

The adhesion energy between bilayers (which is negative) is the sum of the negative attractive energy and positive repulsive energy at the equilibrium fluid spacing. Therefore, compared to phospholipid bilayers such as phosphatidylcholine, the large magnitude of the adhesion energy for GalCer bilayers can either be due to a larger attractive energy or a smaller repulsive energy. However, the following calculation indicates that the latter possibility cannot explain the large adhesion energy for GalCer. By integrating the measured total repulsive pressure for DPPC in the gel phase (*86*), we find that the total repulsive energy for DPPC is approximately 0.1−0.2 erg/cm^2. Since this number is small compared to the adhesion energy of GalCer (-1.5 erg/cm^2), a smaller repulsive pressure could not produce the large adhesion energy observed for GalCer. Therefore, the total attractive pressure must be much larger for GalCer than for DPPC or other PC bilayers.

Calculations of Yu et al. (*35*) based on Lifschitz theory indicate that the incorporation of sugar lipids has a relatively small effect on the attractive van der Waals interaction between bilayers. Yu et al. (*35*) suggested that for LacCer/PC bilayers there must be an additional large, short-range attractive pressure between bilayers to account for the large adhesion energy. Our observation of a *discontinuous* unbinding of GalCer bilayers with increasing DPPG concentration is consistent with the presence of an additional short-range attractive interaction. Yu et al. (*35*) suggest the involvement of hydrogen bonds between sugar groups from apposing bilayers, similar to the proposed H-bond formation between apposing headgroups in hydrated PE bilayers (*14*). In single crystals of GalCer (*55*), each cerebroside molecule participates in eight hydrogen bonds but these H-bonds are all within the same molecular layer. That is, in the cerebroside−ethanol crystals there are no interbilayer H-bonds, although there are H-bonds between the cerebroside and ethanol molecules. However, as noted above, there are marked differences in diffraction patterns from GalCer in ethanol and water, at least keeping open the possibility that there could be interbilayer H-bond formation in hydrated GalCer.

Another possible attractive interaction between GalCer bilayers is hydrophobic packing between galactose moieties from apposing bilayers. In the case of lectin−carbohydrate interactions, evidence has accumulated that there is hydrophobic packing between the hydrophobic face of carbohydrates, particularly galactose, and aromatic amino acids (*87*, *88*). Although carbohydrates are highly polar, they have an

amphipathic character with significant nonpolar patches (*87*, *88*). Therefore, depending on the conformation of the galactose moiety in GalCer bilayers, there could be strong interactions between the hydrophobic galactose surfaces from apposing bilayers.

Biological membranes, such as myelin membranes, which contain large concentrations of cerebrosides, also contain significant amounts of cholesterol so that the membrane lipids are in a liquid-crystalline phase. However, the attractive interactions demonstrated above for gel-phase GalCer bilayers should also operate between GalCer bilayers in the liquid-crystalline phase. For liquid-crystalline bilayers, micropipet measurement studies (*12*) have indeed shown that the adhesion energy of a sugar lipid (digalactosyl diacyl glycerol) is greater than that of liquid-crystalline phase PC or PE.

SUMMARY

In excess water at 20 °C, GalCer forms gel-phase bilayers with hexagonally packed hydrocarbon chains that partially interdigitate across the center of the bilayer. The interbilayer fluid space is extremely narrow (less than 2 Å, or less than the "diameter" of a single water molecule) and the adhesion energy between GalCer bilayers is quite large compared to phosphatidylcholine bilayers. The small fluid space and large adhesion energies are due to a large, short-range attractive interaction between galactose moieties from apposing bilayers.

ACKNOWLEDGMENT

We thank Dr. Eric Toone for useful discussions concerning the energetics of protein−carbohydrate interactions and Dr. Sid Simon for reading a draft of this manuscript and providing very helpful suggestions.

REFERENCES

1. Rand, R. P., and Parsegian, V. A. (1989) *Biochim. Biophys. Acta 988*, 351−376.
2. Leikin, S., Parsegian, V. A., and Rau, D. C. (1993) *Annu. Rev. Phys. Chem. 44*, 369−395.
3. McIntosh, T. J., and Simon, S. A. (1994) *Annu. Rev. Biophys. Biomol. Struct. 23*, 27−51.
4. McIntosh, T. J., and Simon, S. A. (1996) *Colloids Surf. A* 251−268.
5. Israelachvili, J., and Wennerstrom, H. (1996) *Nature 379*, 219−225.
6. LeNeveu, D. M., Rand, R. P., Parsegian, V. A., and Gingell, D. (1977) *Biophys. J. 18*, 209−230.
7. Parsegian, V. A., and Rand, R. P. (1983) *Ann. New York Acad. Sci. 416*, 1−12.
8. Marra, J., and Israelachvili, J. (1985) *Biochemistry 24*, 4608−4618.
9. McIntosh, T. J., and Simon, S. A. (1986) *Biochemistry 25*, 4058−4066.
10. McIntosh, T. J., Magid, A. D., and Simon, S. A. (1987) *Biochemistry 26*, 7325−7332.
11. McIntosh, T. J., Advani, S., Burton, R. E., Zhelev, D. V., Needham, D., and Simon, S. A. (1995) *Biochemistry 34*, 8520−8532.
12. Evans, E., and Needham, D. (1987) *J. Phys. Chem. 91*, 4219−4228.
13. Rand, R. P., Fuller, N., Parsegian, V. A., and Rau, D. C. (1988) *Biochemistry 27*, 7711−7722.
14. McIntosh, T. J., and Simon, S. A. (1996) *Langmuir 12*, 1622−1630.
15. McIntosh, T. J., Simon, S. A., Needham, D., and Huang, C.-h. (1992) *Biochemistry 31*, 2020−2024.
16. Cowley, A. C., Fuller, N. L., Rand, R. P., and Parsegian, V. A. (1978) *Biochemistry 17*, 3163−3168.
17. Loosley-Millman, M. E., Rand, R. P., and Parsegian, V. A. (1982) *Biophys. J. 40*, 221−232.
18. McIntosh, T. J., Magid, A. D., and Simon, S. A. (1990) *Biophys. J. 57*, 1187−1197.
19. McIntosh, T. J., Magid, A. D., and Simon, S. A. (1989) *Biochemistry 28*, 17−25.
20. Marra, J. (1986) *J. Colloid Interface Sci. 109*, 11−20.
21. Israelachvili, J. N., and Wennerstrom, H. (1990) *Langmuir 6*, 873−876.
22. Israelachvili, J. N., and Wennerstrom, H. (1992) *J. Phys. Chem. 96*, 520−531.
23. Harbich, W., and Helfrich, W. (1984) *Chem. Phys. Lipids 36*, 39−63.
24. Helfrich, W., and Servuss, R.-M. (1984) *Il Nuovo Cimento 3*, 137−151.
25. Evans, E. A., and Parsegian, V. A. (1986) *Proc. Natl. Acad. Sci. U.S.A. 83*, 7132−7136.
26. Kojima, N., and Hakomori, S.-I. (1989) *J. Biol. Chem. 264*, 20159−20162.
27. Kojima, N., and Hakomori, S.-I. (1991) *J. Biol. Chem. 266*, 17552−17558.
28. Yamada, K. M., Critchley, D. R., Fishman, P. H., and Moss, J. (1983) *Exp. Cell Res. 143*, 295−302.
29. Curatolo, W. (1987) *Biochim Biophys Acta 906*, 137−160.
30. Haywood, A. M. (1974) *J. Mol. Biol. 83*, 427−436.
31. van Heyningen, S. (1974) *Science 183*, 656−657.
32. Curatolo, W., Yau, A. O., Small, D. M., and Sears, B. (1978) *Biochemistry 17*, 5740−5744.
33. Hakomori, S.-I. (1993) *Bichem. Soc. Trans. 21*, 583−595.
34. McIntosh, T. J., and Simon, S. A. (1994) *Biochemistry 33*, 10477−10486.
35. Yu, Z. W., Calvert, T. L., and Leckband, D. (1998) *Biochemistry 37*, 1540−1550.
36. Bosio, A., Binczek, E., and Stoffel, W. (1996) *Proc. Natl. Acad. Sci. U.S.A. 93*, 13280−13285.
37. Coetzee, T., Fujitsa, N., Dupree, J., Shi, R., Blight, A., Suzuki, K., and Popko, B. (1996) *Cell 86*, 209−219.
38. Bosio, A., Binczek, E., Haupt, W. F., and Stoffel, W. (1998) *J. Neurochem. 70*, 308−315.
39. Dupree, J., Coetzee, T., Blight, A., Suzuki, K., and Popko, B. (1998) *J. Neuorsci. 18*, 1642−1649.
40. Hakomori, S., Igarashi, Y., Kojima, N., Okoshi, K., Handa, B., and Fenderson, B. (1991) *Glycoconjugate J. 8*, 178−192.
41. Stewart, R. J., and Boggs, J. M. (1993) *Biochemistry 32*, 10666−10674.
42. Koshy, K. M., Wang, J., and Boggs, J. M. (1999) *Biophys. J. 77*, 306−318.
43. Harouse, J. M., Bhat, S., Spitalnik, S. L., Laughlin, M., Stefano, K., Silberberg, D. H., and Gonzalez-Scarano, F. (1991) *Science 253*, 320−323.
44. Reiss-Husson, F. (1967) *J. Mol. Biol. 25*, 363−382.
45. Ruocco, M. J., and Shipley, G. G. (1983) *Biochim Biophys Acta 735*, 305−308.
46. Curatolo, W., and Jungalwala, F. B. (1985) *Biochemistry 24*, 6608−6613.
47. Maggio, B., Ariga, T., Sturtevant, J. M., and Yu, R. K. (1985) *Biochemistry 24*, 1084−1092.
48. Ruocco, M. J., Atkinson, D., Small, D. M., Skarjune, R. P., Oldfield, E., and Shipley, G. G. (1981) *Biochemistry 21*, 5957−5966.
49. Ruocco, M. J., Shipley, G. G., and Oldfield, E. (1983) *Biophys. J. 43*, 91−101.
50. Bunow, M. R., and Levin, I. W. (1988) *Biochim. Biophys. Acta 939*, 577−586.
51. Reed, R. A., and Shipley, G. G. (1989) *Biophys. J. 55*, 281−292.
52. Haas, N. S., and Shipley, G. G. (1995) *Biochim. Biophys. Acta 1240*, 133−141.
53. Skarjune, R., and Oldfield, E. (1979) *Biochim. Biophys. Acta 556*, 208−218.
54. Lee, D. C., Miller, I. R., and Chapman, D. (1986) *Biochim. Biophys. Acta 859*, 266−270.

55. Pascher, I., and Sundell, S. (1977) *Chem. Phys. Lipids 20*, 175−191.
56. Nyholm, P.-G., Pascher, I., and Sundell, S. (1990) *Chem. Phys. Lipids 52*, 1−10.
57. Pink, D. A., MacDonald, A. L., and Quinn, B. (1988) *Chem. Phys. Lipids 47*, 83−95.
58. Bunow, M. R., and Levin, I. W. (1980) *Biophys. J. 32*, 1007−1022.
59. Stinson, R. H., and Boggs, J. M. (1989) *Biochim. Biophys. Acta 986*, 234−240.
60. Abrahamsson, S., Pascher, I., Larsson, K., and Karlsson, K.-A. (1972) *Chem. Phys. Lipids 8*, 152−179.
61. Skarjune, R., and Oldfield, E. (1982) *Biochemistry 21*, 3154−3160.
62. Gruner, S., Lenk, R. P., Janoff, A. S., and Ostro, M. J. (1985) *Biochemistry 24*, 2833−2842.
63. Parsegian, V. A., Fuller, N., and Rand, R. P. (1979) *Proc. Natl. Acad. Sci. U.S.A. 76*, 2750−2754.
64. O'Brien, F. E. M. (1948) *J. Sci. Instrum. 25*, 73−76.
65. Parsegian, V. A., Rand, R. P., Fuller, N. L., and Rau, R. C. (1986) *Methods Enzymol. 127*, 400−416.
66. Blaurock, A. E., and Worthington, C. R. (1966) *Biophys. J. 6*, 305−312.
67. Herbette, L., Marquardt, J., Scarpa, A., and Blasie, J. K. (1977) *Biophys. J. 20*, 245−272.
68. Shannon, C. E. (1949) *Proc. Inst. Radio Engrs., N.Y. 37*, 10−21.
69. McIntosh, T. J., and Holloway, P. W. (1987) *Biochemistry 26*, 1783−1788.
70. Tardieu, A., Luzzati, V., and Reman, F. C. (1973) *J. Mol. Biol. 75*, 711−733.
71. Blaurock, A. E., and McIntosh, T. J. (1986) *Biochemistry 25*, 299−305.
72. Watts, A., Harlos, K., and Marsh, D. (1981) *Biochim. Biophys. Acta 645*, 91−96.
73. Curatolo, W. (1982) *Biochemistry 21*, 1761−1764.
74. McIntosh, T. J., and Simon, S. A. (1986) *Biochemistry 25*, 4948−4952.
75. Lesslauer, W., Cain, J. E., and Blasie, J. K. (1972) *Proc. Natl. Acad. Sci. U.S.A. 69*, 1499−1503.
76. Janiak, M. J., Small, D. M., and Shipley, G. G. (1979) *J. Biol. Chem. 254*, 6068−6078.
77. Wiener, M. C., Suter, R. M., and Nagle, J. F. (1989) *Biophys. J. 55*, 315−325.
78. Nabet, A., Boggs, J. M., and Pezolet, M. (1996) *Biochemistry 35*, 6674−6683.
79. Grant, C. W. M., Mehlhorn, I. E., Florio, E., and Barber, K. R. (1987) *Biochim. Biophys. Acta 902*, 169−177.
80. Mehlhorn, I. E., Florio, E., Barber, K. R., Lordo, C., and Grant, C. W. M. (1988) *Biochim. Biophys. Acta 939*, 151−159.
81. Mason, J. T., Huang, C.-h., and Biltonen, R. L. (1981) *Biochemistry 20*, 6086−6092.
82. Huang, C.-h., and Mason, J. T. (1986) *Biochim. Biophys. Acta 864*, 423−470.
83. Cevc, G. (1990) *Biochim. Biophys. Acta 1031*, 311−382.
84. Israelachvili, J. (1992) *Intermolecular and Surface Forces*, 213−249, Academic Press, London.
85. McLaughlin, S. (1989) *Annu. Rev. Biophys. Biophys. Chem. 18*, 113−136.
86. McIntosh, T. J., and Simon, S. A. (1993) *Biochemistry 32*, 8374−8384.
87. Weis, W. I., and Drickamer, K. (1996) *Annu. Rev. Biochem. 65*, 441−473.
88. Gabius, H.-J. (1998) *Pharm. Res. 15*, 23−30.

BI991725M